

# Hydrophobic hydration around a pair of apolar species in water<sup>a)</sup>

C. Pangali,<sup>b)</sup> M. Rao, and B. J. Berne

Department of Chemistry, Columbia University, New York, New York 10027  
(Received 7 May 1979; accepted 21 June 1979)

The structure of ST2 water around a pair of spherical nonpolar (Lennard-Jones) particles,  $A_1-A_2$ , is studied as a function of pair separation,  $r$ , using a force-bias Monte Carlo technique with importance sampling. The change in the water structure (or equivalently the hydrophobic hydration) is correlated with the potential of mean force,  $W_{AA}(r)$ , determined in a previous study. It is found that the second minimum in  $W_{AA}(r)$  corresponds to a water molecule lying between the two apolar particles. The water always maintains a "linear hydrogen bond" network and is more ordered in the neighborhood of the two spheres except possibly when they are separated by a distance corresponding to the position of the free energy barrier, that is the maximum in  $W_{AA}(r)$ .

## I. INTRODUCTION

Hydrophobic effects are thought to be responsible for the stability of particular conformations of large molecules in aqueous solutions, and for the existence of such interesting states of aggregation of amphiphilic molecules as micelles and bilipid membranes.<sup>1</sup> It is convenient to divide hydrophobic effects into two classes. Hydrophobic hydration refers to the structure of the water molecules in the immediate neighborhood of the apolar solute molecules; and to the thermodynamic properties of very dilute solutions. This is the subject of the present paper. Hydrophobic interaction on the other hand refers to the solvent induced interaction between two or more apolar solute molecules. This was the subject of a preceding paper.<sup>2</sup> Hydrophobic hydration is readily observed experimentally, but because apolar species are exceedingly insoluble in water, hydrophobic interactions are not amenable to direct experiment. Many investigators have therefore tried to infer details of the hydrophobic interaction from solubility data; that is, from hydrophobic hydration.<sup>3,4</sup> This kind of analysis has recently been called into question. Nevertheless, it is the hydrophobic interaction that lies at the root of important phenomena, and it is thus of extreme importance to better understand this phenomenon. This is an area where computer simulation can provide answers that are not otherwise available.

The low solubility of apolar species in aqueous solutions can be attributed to the fact that the water molecules neighboring the solute must rearrange themselves in order to maintain a complete hydrogen bond network. This rearrangement leads to a substantial decrease in the entropy of the water. It is this negative entropy change which gives rise to a decrease in the solubility with increasing temperature for temperatures between 15 and 25°C. Considerations of this sort have led

Frank and Evans<sup>7</sup> to propose an "iceberg" model for the hydration of nonpolar solutes in which the water surrounding the solute is more structured than is bulk water. These effects are dramatically illustrated by the standard entropy of solution for KCl in water and for Ar in water at 298°K.

$$\Delta S_{\text{KCl}}^\circ = -51.9 \text{ cal/mole deg,}$$

$$2\Delta S_{\text{Ar}}^\circ = -60.4 \text{ cal/mole deg.}$$

While the entropy change for KCl does not appear surprising when seen in the light of the structure promoting effect of ions on the water molecules, the magnitude of  $\Delta S_{\text{Ar}}^\circ$  is certainly unexpected. Unlike an ion, the interaction of Ar atoms with water is certainly weak. Although a small part of  $\Delta S_{\text{Ar}}^\circ$  arises from restricting the Ar atoms to a cage of water molecules, much of the entropic change actually results from a restructuring of the solvent surrounding the Ar atom. Experimental data on such structure enhancement comes from a wide variety of sources: NMR relaxations,<sup>5</sup> dielectric relaxation,<sup>6</sup> etc. The most widely held view of the structure of aqueous solutions is that the apolar species reside in a polyhedral cage of water molecules—rather in the spirit of the solid clathrate hydrates. Of course, it is understood that the cages are not as rigid as in the solid.

The hydrophobic interaction has been the subject of much discussion.<sup>1-4</sup> The usual view is based on simple ideas. Because nonpolar species are relatively insoluble in water, it is assumed that there are thermodynamic forces that will drive two such species together to a much greater extent than would be the case if these solutes were dissolved in a more accommodating solvent. If  $g_{AA}(r)$  denotes the pair correlation function of two spherical nonpolar species (A particles) dissolved in water, then the potential of mean force

$$W_{AA}(r) \equiv -kT \ln g_{AA}(r)$$

is a good measure of the solvent induced interactions between the two particles.  $W_{AA}(r)$  is the reversible work required to bring the two particles from infinite separation ( $r = \infty$ ) to  $r$ . In a constant volume ensemble ( $N, V, T$ ),  $W_{AA}(r)$  corresponds to  $\Delta A_{AA}(r)$ , the Helmholtz free energy change for the process.

<sup>a)</sup>This work was supported by grants from the National Science Foundation (NSF CHE 76-11002) and the National Institute of Health (NIH RO1 NS 12714-03).

<sup>b)</sup>In partial fulfillment of the Ph. D. in Chemistry at Columbia University. C. Pangali's present address is Department of Chemistry, Harvard University, Cambridge, Mass. 02138.

In the preceding paper<sup>2</sup> we computed  $W_{AA}(r)$  for a model of two Lennard-Jones spheres of diameter  $\sigma_{AA} = 4.12 \text{ \AA}$  "dissolved" in 214 ST2 water molecules at 298 °K and a water density of  $1 \text{ gm cm}^{-3}$ , and found that  $W_{AA}(r)$  exhibited oscillations. The magnitudes of the maxima and minima and their positions are consistent with the view that there are two relatively stable positions for the A-A pair. In one position the A spheres are nearly touching whereas in the other position they are separated by a water molecule. The maximum separating these two positions can be interpreted as a barrier to the transition from A-A to A-(H<sub>2</sub>O)-A. One possible interpretation of these results is that the conventional view of the hydrophobic interaction is qualitatively wrong. From our computed  $g_{AA}(r)$  it can be shown that of these relatively stable states, the conformation A-(H<sub>2</sub>O)-A is relatively more probable. For a detailed discussion of these results and for a comparison with the recent theory of Pratt and Chandler,<sup>8</sup> the reader should see Ref. 2.

In this paper we study the structure of the water molecules around the two A particles as a function of the distance between them. We show that the hydrophobic hydration depends on the distance between the A particles in an important way.

This study is made using the force-bias Monte Carlo technique<sup>9</sup> with importance sampling in the  $(N, V, T)$  ensemble for the same system studied in Ref. 2; that is, for two Lennard-Jones spheres ( $\epsilon_{AA}/k = 179 \text{ }^\circ\text{K}$ ,  $\sigma_{AA} = 4.12 \text{ \AA}$ ) dissolved in 214 ST2 water molecules at  $T = 298 \text{ }^\circ\text{K}$  and a mass density of  $1 \text{ gm cm}^{-3}$ . Each sphere interacts with each water molecule with an L-J potential ( $\epsilon_{AW}/k = 77.82 \text{ }^\circ\text{K}$ ,  $\sigma_{AW} = 3.43 \text{ \AA}$ ) and the simulation was carried out with periodic boundary conditions using a spherical cutoff with truncation distance of  $8.46 \text{ \AA}$ .

Several computer studies have recently appeared on the topic of hydration of apolar species. Geiger *et al.*<sup>10</sup> studied a pair of neon atoms dissolved in 214 ST2 water molecules by the molecular dynamics method. The neon atoms were initially placed in contact, and stayed there for some time before jumping apart and settling into separate cages with a molecule of water separating them. This study sheds some new light on the arrangement of water molecules vicinal to the apolar species. Owicki and Scheraga<sup>11</sup> carried out a Monte Carlo study of a single methane molecule dissolved in 100 water molecules. They used the isothermal-isobaric  $(T, P, N)$  ensemble. More recently, Swaminathan *et al.*<sup>12</sup> have carried out a Monte Carlo simulation in the  $(N, V, T)$  ensemble of a single methane molecule in water interacting with potential function determined from *ab initio* quantum mechanical calculations.

Our work differs considerably from Owicki and Scheraga's<sup>11</sup> and from Swaminathan *et al.*,<sup>12</sup> because we study hydrophobic hydration near two spheres whereas they study it near only one sphere. Our work is similar in spirit to that of Geiger *et al.*<sup>10</sup> However, because importance sampling was not used in their molecular dynamics simulation, many of the important structural features could not be studied in those im-

portant regions. Our work complements the work of Geiger *et al.*<sup>10</sup> and leads to several important conclusions.

We note in passing that there are still some fundamental problems in simulating water due to boundary conditions, the potential model, etc. These are discussed at great length in several recent publications.<sup>13-15</sup> The results of all computer simulations should, like the results reported here, be viewed with a certain healthy skepticism.

## II. METHOD

The system discussed here consists of  $N = 216$  particles of which  $N_w = 214$  are ST2<sup>9</sup> water molecules and  $N_A = 2$  are the pair of apolar species. The interaction potential for the  $N$  particles is given by

$$U'_N(\mathbf{R}_N) = \sum_{j>i}^{N_w} \Phi_{ij} + \sum_{i=1}^{N_A} \sum_{j=1}^{N_w} \Phi_{LJ}(r_{ij}) + \Phi(r_{AA}) + U_H(r_{AA}) \quad (2.1)$$

$$\equiv U_N(\mathbf{R}_N) + U_H(r_{AA}), \quad (2.2)$$

where  $\Phi_{ij}$  is the ST2 pair interaction<sup>16</sup> and  $\Phi_{LJ}(r_{ij})$  is the interaction between a molecule of water and the apolar species.

$$\Phi_{LJ}(r_{ij}) = 4\epsilon_{AW} \left\{ \left( \frac{\sigma_{AW}}{r_{ij}} \right)^{12} - \left( \frac{\sigma_{AW}}{r_{ij}} \right)^6 \right\}, \quad (2.3)$$

where  $\epsilon_{AW}/k = 77.82 \text{ }^\circ\text{K}$  and  $\sigma_{AW} = 3.43 \text{ \AA}$ . The direct interaction between the two apolar species labeled A, A is represented by the last two terms in Eq. (2.1).  $\Phi(r_{AA})$  is the (12-6) Lennard-Jones potential with parameters  $\epsilon_{AA}/k = 170.1 \text{ }^\circ\text{K}$  and  $\sigma_{AA} = 4.12 \text{ \AA}$ .  $U_H(r_{AA})$  is a harmonic potential between the two apolar species,

$$U_H(r_{AA}) = \frac{1}{2} k_0 (r_{AA} - r_{AA}^0)^2, \quad (2.4)$$

where  $k_0$  is a force constant.  $U_H(r_{AA})$  is introduced to restrict the range of  $r_{AA}$  to a small value around pre-selected values of  $r_{AA}^0$ . It should be noted that  $U_H$  does not bind these particles to fixed points in the box. The center of mass of the two spheres is allowed to wander freely within the box, but the two particles move relative to each other in a spherical shell of thickness prescribed by the value of  $k_0$  and of radius fixed at  $r_{AA}^0$ . The computer simulation is carried out for several different values  $r_{AA}^0$ . Apart from this extra constraining potential  $U_H$ , the potential model used here is identical to that used in previous molecular dynamics studies.<sup>17</sup>

The total potential energy is subdivided into a part  $U_N(\mathbf{R}_N)$  and  $U_H(\mathbf{r}_{AA})$ , where  $\mathbf{R}_N$  is the  $(6N_w + 6)$  dimensional vector specifying the positions and orientations of the  $N_w$  rigid water molecules and the two apolar species.

The Monte Carlo simulation generates a walk in configuration space such that the sequence of configurations is distributed according to the Boltzmann distribution. For the potential given by Eq. (2.2) the Boltzmann distribution is  $Q^{-1} e^{-\beta U'}$ , where  $U' = U_N + U_H$ . In this study the temperature is set at  $T = 298 \text{ }^\circ\text{K}$ . What is wanted, however, are ensemble averages of proper-

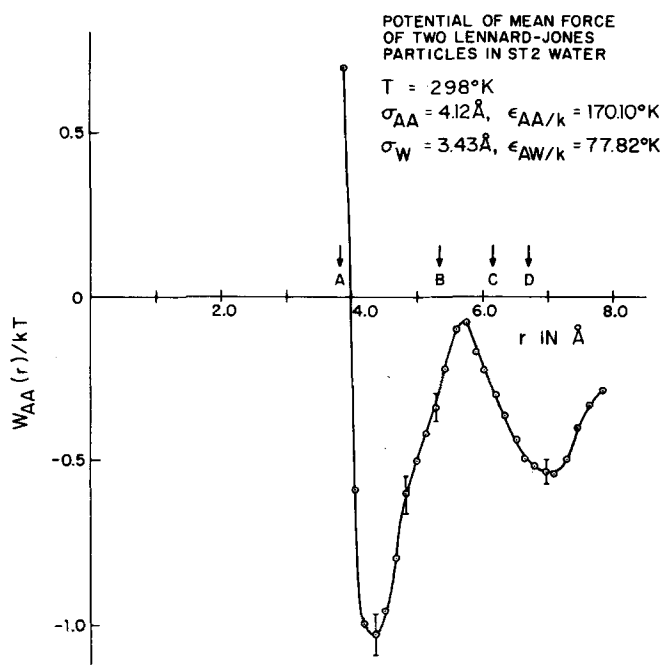


FIG. 1. The potential of mean force obtained from a simulation of two Lennard-Jones particles dissolved in water. The initial separations  $r_{ab}^0$  of the two apolar species are (in Å): 3.87 for A, 5.27 for B, 6.08 for C, and 6.60 for D.

ties  $A$  in an ensemble for which the potential is  $U = U_N(\mathbf{R}_N)$ ; that is, one in which the constraining potential is removed,

$$\langle A \rangle = \int d\mathbf{R}_N A(\mathbf{R}_N) e^{-\beta U_N(\mathbf{R}_N)} / \int d\mathbf{R}_N e^{-\beta U_N(\mathbf{R}_N)}. \quad (2.5)$$

By adding and subtracting  $U_H$  in the exponents, Eq. (2.5) can be expressed as

$$\langle A \rangle = \langle A e^{\beta U_H(\mathbf{r}_{AA})} \rangle_H / \langle e^{\beta U_H(\mathbf{r}_{AA})} \rangle_H,$$

where  $\langle \rangle_H$  denotes an average over the ensemble with the potential energy  $U_N(\mathbf{R}_N) + U_H(\mathbf{r}_{AA})$ , that is, where  $U_H$  is switched on, whereas  $\langle \dots \rangle$  denotes an average over an ensemble with  $U_H$  switched off. Since a set of  $\tau$  configurations labeled  $i = 1, \dots, \tau$  are generated in the MC walk, the ensemble average required is given by

$$\langle A \rangle = \sum_{i=1}^{\tau} A_i e^{\beta U_{Hi}} / \sum_{i=1}^{\tau} e^{\beta U_{Hi}}$$

where  $A_i$  and  $U_{Hi}$  are the values of  $A(\mathbf{R}_N)$  and  $U_H(\mathbf{r}_{AA})$  at the  $i$ th configuration.

The reason for introducing  $U_H$  was to prevent the apolar species from drifting too far apart (see Ref. 2). Of course, the ensemble averages  $\langle A \rangle_H$  could be reported, but we are not interested in pairs of apolar species held together by a harmonic potential.

The Monte Carlo walk was performed using the force-bias procedure (see Ref. 9) with parameters for the translational and orientational steps for water molecules set as follows:  $\Delta r = 0.6$  Å,  $\Delta \theta = 0.898$  rad and  $T = 298$  °K and the density of water was  $1 \text{ g cm}^{-3}$ . The solute particles were moved with smaller steps  $\Delta r$

$= 0.06$  Å. The center of mass of the A-A pair was not held fixed in the box because this would impose an unnecessary constraint on the system. Four separate runs were performed to study small regions  $\Delta r_{AA} \sim 1.0$  Å (or windows) centered around initial A-A separations of  $r_{AA}^0 = 3.88, 5.33, 6.08, 6.60$  Å. These cases are labeled A, B, C, and D respectively. For convenience these separations are indicated along with the potential of mean force in Fig. 1. The starting configurations for these cases were taken from a molecular dynamics study described elsewhere.<sup>17</sup> Each run was further equilibrated for 500 passes, after which averages were taken over a walk of 5000 passes (1 080 000 configurations) for each window.

### III. STRUCTURAL ANALYSIS

It is expected that the distribution of water molecules around the pair of apolar species A-A will depend on the relative separation of the pair,  $r_{AA}$ . To see this we determined the radial distribution of oxygen atoms around each of the A particles. The resulting radial pair correlation function,  $g_{AO}(r)$ , tabulated in Table I, shows how the oxygen distribution does indeed change in response to different A-A pair separations. It is worth noting that the Pratt-Chandler<sup>8</sup> theory can be extended to give this function. It would be of interest to

TABLE I. The total radial distribution function  $g_{AO}(r)$  for the cases A, B, C, D respectively as discussed in the text.

$r$ (Å)	A	B	C	D
2.73	0.003	0.001	0.000	0.009
2.93	0.161	0.145	0.196	0.145
3.13	0.917	0.735	1.065	0.722
3.33	1.559	1.297	1.946	1.688
3.54	1.985	1.734	2.141	2.045
3.74	1.980	1.616	2.182	1.879
3.94	1.679	1.531	1.777	1.650
4.14	1.410	1.363	1.428	1.387
4.34	1.065	1.111	1.186	1.230
4.55	0.871	1.064	0.893	1.102
4.75	0.717	0.901	0.826	0.974
4.95	0.636	0.863	0.759	0.851
5.15	0.729	0.844	0.662	0.765
5.35	0.702	0.774	0.616	0.754
5.56	0.698	0.769	0.656	0.791
5.76	0.776	0.873	0.728	0.881
5.96	0.936	0.965	0.865	1.018
6.16	1.070	1.011	1.030	1.116
6.36	1.175	1.060	1.099	1.105
6.57	1.083	1.098	1.112	1.069
6.77	1.126	1.043	1.024	0.987
6.97	1.131	1.016	1.065	0.967
7.17	1.119	1.031	1.043	0.939
7.37	1.096	1.074	1.091	0.969
7.58	1.115	1.071	1.076	1.012
7.78	1.054	1.075	1.068	1.034
7.98	1.037	1.057	1.016	1.029
8.18	1.012	1.071	1.051	1.072
8.38	1.022	1.068	1.052	1.088
8.59	1.025	1.045	1.051	1.030
8.79	1.015	1.067	1.044	1.052
8.99	1.010	1.042	1.026	1.070
9.19	1.067	1.029	1.034	1.032

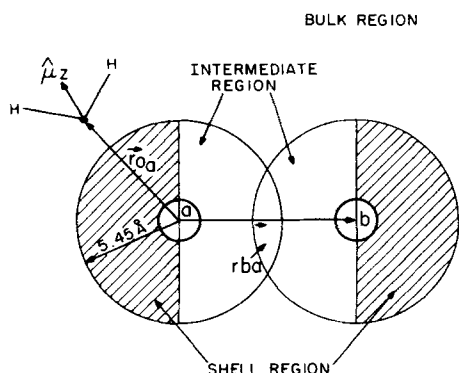


FIG. 2. Illustration of the division of solvent molecules into the shell, bulk, and intermediate regions. The vector  $\hat{U}_z$  lies in the plane of HOH and bisects the angle HOH.

see whether that theory, which we have shown to be in excellent agreement with our simulations<sup>2</sup> with regard to the potential of mean force, would also give the solvent structure accurately.

To better understand the solvent structure it is useful to divide the space around the two apolar species into an interior and an exterior region as shown in Fig. 2. The exterior region is defined as the hemispheres around each apolar particle that points away from the other particle. This condition is met by

$$\mathbf{r}_{0a} \cdot \mathbf{r}_{ba} \leq 0, \quad (3.1a)$$

and

$$\mathbf{r}_{0b} \cdot \mathbf{r}_{ab} \leq 0, \quad (3.1b)$$

where  $\mathbf{r}_{ji} = \mathbf{r}_j - \mathbf{r}_i$ . Equation (3.1a) defines the exterior region around particle  $a$  whereas Eq. (3.1b) defines the exterior region around particle  $b$ . The interior regions with respect to particles  $a$  and  $b$ , respectively, are defined by

$$\mathbf{r}_{0a} \cdot \mathbf{r}_{ba} > 0, \quad (3.1c)$$

$$\mathbf{r}_{0b} \cdot \mathbf{r}_{ab} > 0. \quad (3.1d)$$

This division of space allows us to determine the apolar-oxygen radial pair correlation function exterior and interior to an apolar species. These functions are given in Fig. 3. The line passing through the open circles gives the exterior pair correlation functions whereas a dashed line through crosses gives the interior correlation function. The sum of these two functions gives the total  $g_{AO}(r)$  given in Table I. In addition the running coordination number  $n_{AO}(r)$ , defined by

$$n_{AO}(r) = 4\pi\rho_w \int_0^r ds s^2 g_{AO}(s), \quad (3.2)$$

with  $\rho_w$  denoting the number density of water is also given in Fig. 3. The dashed line gives the interior coordination number whereas the solid line gives the exterior coordination number.

Let us first consider the exterior radial distribution,  $g_{AO}^{\text{Ext}}(r)$ . The first hydration shell is quite broad (Fig. 3) stretching from  $\sim 2.90$  Å to  $\sim 5.45$  Å. In contrast the first peak of  $g_{OO}(r)$  for ST2 water (see Fig. 4) at

$T = 283$  °K spans a narrow range from  $\sim 2.80$  Å to  $\sim 3.50$  Å with the coordination number  $n_{AO} = 5.7$  at  $r = 3.50$  Å. The number of water molecules in the hydration shell of the apolar species  $n_{AO}(r)$  is evaluated at  $r = 5.45$  Å is 20.28, 19.87, 20.09, and 20.48 respectively for each of the cases A, B, C and D. The height of the first peak is  $\sim 2.20 \pm 0.2$  in all four cases, in reasonable agreement with the Stillinger scaled particle theory.<sup>18</sup>

Any statement about the structure of the hydration shells around an A particle is predicted on the accuracy of  $g_{AO}^{\text{Ext}}(r)$ : Since there are only two A particles, the function  $g_{AO}^{\text{Ext}}(r)$  is computed using  $2N_w$  pair distances. This should be contrasted with the functions  $g_{OO}(r)$  where  $N_w(N_w - 1)/2$  pair distances are used. Clearly  $g_{OO}(r)$  will be determined to greater accuracy than  $g_{AO}(r)$ . To gain some insight into the relative errors we computed  $g_{OO}(r)$  for neat water consisting of 216 ST2 water molecules at  $T = 283$  °K and  $\rho = 1$  gm cm<sup>-3</sup>. Two different methods were used to compute  $g_{OO}(r)$ . In the first method two water molecules were selected and the radial distribution of the other water molecules with respect to these two were used to determine  $g_{OO}(r)$ .

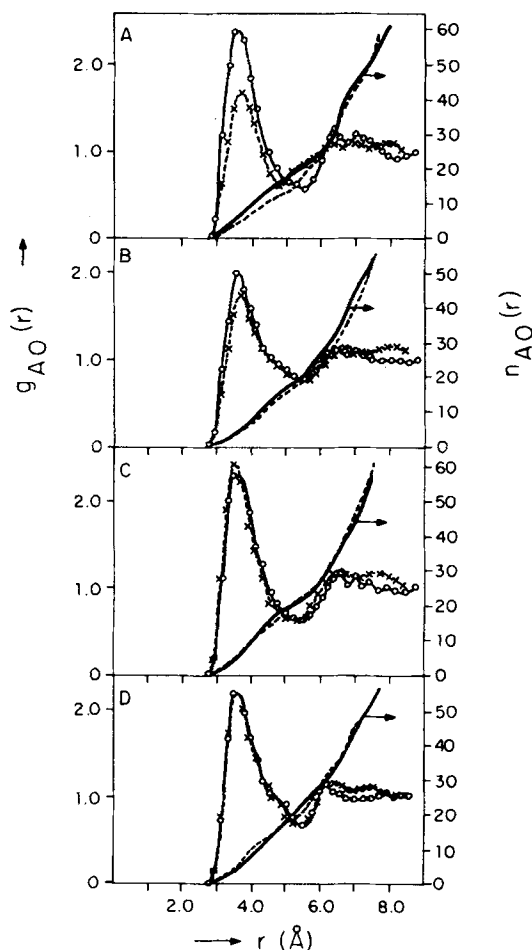


FIG. 3. The calculated apolar species-oxygen correlation functions for the four cases A, B, C, and D. Also shown are running coordination numbers  $n_{AO}(r)$ . The full lines give the exterior functions and the dashed lines give the interior functions discussed in the text.

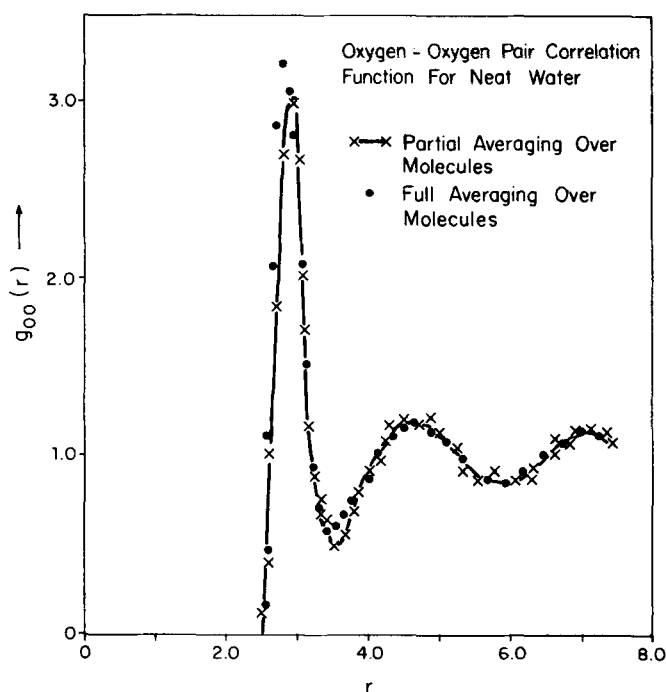


FIG. 4. The oxygen-oxygen pair correlation functions determined from a simulation of 216 ST2 molecules at  $T=283^\circ\text{K}$ . The crosses (x) denote the function determined by a partial averaging over only two oxygen atoms at the origin, while the circles denote the function from a full averaging over all molecules. This comparison serves to illustrate the magnitude of the errors in Fig. 1 arising from the averaging over only two solute particles. It also demonstrates that partial averaging for this system gives an adequate representation of the exact function; in particular, no manifestation of quasi-ergodicity is observed.

This function is determined in an analogous manner to  $g_{\text{AO}}(r)$ . The same number of MC passes were used here as in the determination of  $g_{\text{AO}}(r)$ . In the second method  $g_{\text{OO}}(r)$  was determined for the same number of passes, but averaging over all  $N_{\text{W}}$  water molecules. This is the standard method. The two resulting  $g_{\text{OO}}(r)$  functions are compared in Fig. 4 where it can be seen that the partial averaging yields a function remarkably close to the exact function.

Returning now to Fig. 3, it is interesting that the shoulder observed by Geiger *et al.*<sup>10</sup> in  $g_{\text{AO}}(r)$  at  $r \approx 4.0 \text{ \AA}$  is not present in this study. However, a small valley in the second peak of  $g_{\text{AO}}^{\text{Ext}}(r)$ , around  $\sim 6.5 \text{ \AA}$ , is found to varying degrees for cases A, B, and C. A similar structure was observed by Owicki and Scheraga in their MC study of a single apolar species in water.

One final point about  $g_{\text{AO}}^{\text{Ext}}(r)$ . The region B is centered around the maximum in the potential of mean force for the two apolar species (see Ref. 2). Since this is an unstable position we expect and find that  $g_{\text{AO}}(r)$  for B shows a greater width than the corresponding function for A, C, and D.

The correlations of the apolar species with the exterior hydrogens are shown in Fig. 5, defined by the

restriction  $\mathbf{r}_{\text{Ha}} \cdot \mathbf{r}_{\text{ba}} \leq 0$ . The presence of the second apolar species does not unduly affect these correlation functions. An interesting feature of the  $g_{\text{AH}}(r)$  is the shoulder at  $\sim 4.2 \text{ \AA}$  in cases A, C, and D. Owicki and Scheraga<sup>7</sup> also observed a similar structure in their  $g_{\text{AH}}(r)$ . The first peak of  $g_{\text{AH}}(r)$ , like the first peak of  $g_{\text{AO}}(r)$ , is rather broad, while the second peak is narrower and not well defined.

The first peak in  $g_{\text{AH}}(r)$  occurs at  $\sim 3.30 \text{ \AA}$ ; taken with the fact that the first peak in  $g_{\text{AO}}(r)$  is located at  $3.6 \text{ \AA}$ , this suggests that the oxygen-proton bonds in the immediate vicinity of the apolar species point parallel to the surface of the apolar species. This is exactly what one expects from a cage-like structure of the water molecules around the apolar entities. It is worth noting that while in the first shell of water molecules around the apolar species the protons are slightly closer to the apolar species than the oxygens ( $3.30 \text{ \AA}$  vs  $3.60 \text{ \AA}$ ), the converse is true for the second shell ( $6.5$  vs  $6.0 \text{ \AA}$ ). This suggests that the second shell water molecules act as electron donors to the first shell water molecules.

The foregoing functions were computed for the "exterior" water molecules indicated in the shaded hemispherical regions of Fig. 2. The behavior of the water molecules in this region is quite similar to the water mole-

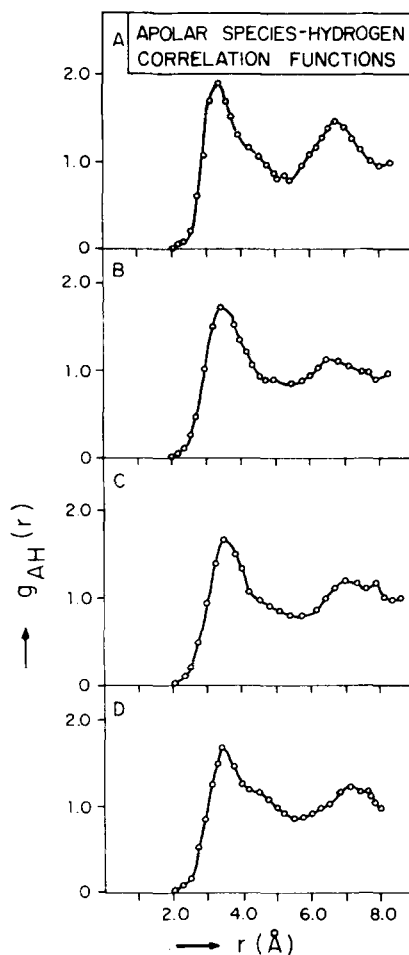


FIG. 5. The apolar species-hydrogen correlation functions. The labels A, B, C, and D are defined in the caption to Fig. 1.

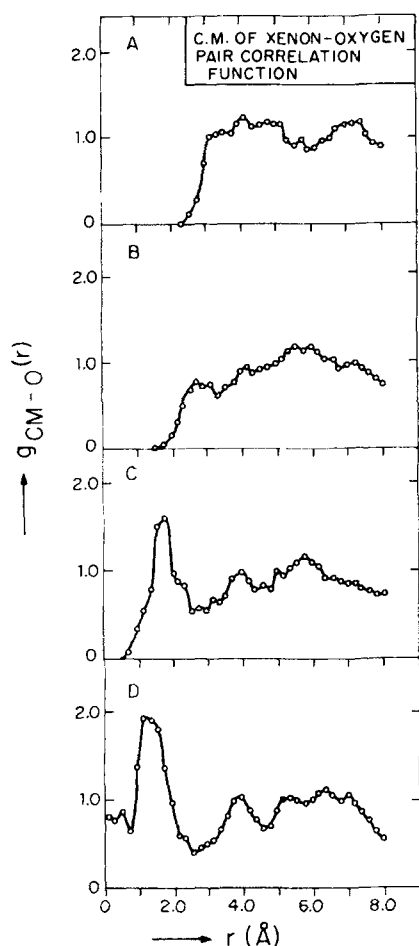


FIG. 6. The center of mass of xenon-oxygen pair correlation function. The labels A, B, C, D are same as in Fig. 1.

cules in the hydration shells of a single nonpolar species dissolved in water. We expect the water molecules in the intermediate region to behave differently. For reference, the radial distribution function of the water molecules located to the right of the leftmost A particle or to the left of the rightmost A particle in Fig. 2 was also computed. This contains information about the interior water molecules. These functions are compared to the corresponding functions for the exterior waters in Fig. 3. The first peak in this function changes drastically when one goes from configurations A to B, C, D, indicating that a water molecule is penetrating into the region interior to both A particles in these latter configurations. The second peak is much broader for configuration A than for the other configurations because the second A particle screens the first A particle from some of the water molecules.

To further study the interior water molecules it is useful to determine the radial distribution function of the oxygen atoms with respect to the center of mass of the two A particles. This function is denoted  $g_{\text{C.M.}-\text{O}}(r)$  and it is presented in Fig. 6 for the different pair separations of the A-A particles. Figure 6 clearly shows that the penetration of water molecules into the region between the two A particles increases as the A-A pair separation is increased. One very interesting feature is

that only when the A-A separation corresponds to the second minimum (separation D) in the potential of mean force (cf. Fig. 1) can an oxygen atom be found directly between the two A particles. In all other configurations  $g_{\text{C.M.}-\text{O}}(r)$  is zero at the c.m. For separation B and C corresponding to the barrier in the potential of mean force, the  $g_{\text{C.M.}-\text{O}}(r)$  shows strikingly different distributions with respect to the c.m. In the separation C there is a sharp peak which probably corresponds to water molecules distributed in the "pinched region" in the excluded volume of the two A particles. In separation B this pinched region is too small to give a repository for water molecules.

#### IV. ENERGY CONSIDERATIONS

It is generally accepted that the low solubility of nonpolar substances in water is due mainly to the negative entropy change accompanying such a process. The measured enthalpies of solution are in fact generally exothermic but very small compared to  $|T\Delta S|$ . We attempt to understand these factors by analyzing the changes in binding energy of the water molecules that occur when dissolution of nonpolar groups takes place in water. All the ensemble averages discussed in this section are determined as indicated in Sec. II, unless otherwise noted.

The average solvation energy of the apolar species is defined as

$$\langle e_{\text{solv}} \rangle = \left\langle \left( \frac{1}{2} \sum_{i=1}^2 \sum_{j=1}^{N_W} \Phi_{Lj}(r_{ij}) \right) \right\rangle \quad (4.1)$$

In Eq. (4.1) the sum over  $j$  is restricted to those water molecules lying within a radius  $r_c$  of each apolar species ( $i=1, 2$ ). In Table II we see that as the separation between the two apolar species is increased,  $\langle e_{\text{solv}} \rangle$  increases in magnitude, finally converging to  $-13.06\epsilon$  ( $\approx 1$  kcal/mole). This is understandable since the number of apolar-water interactions grows with increasing separation of the apolar species, and finally converges to a constant number of interactions.

Let the binding energy of particle  $j$  be  $\epsilon_j$ , that is,

$$\epsilon_j = \sum_{\substack{i=1 \\ i \neq j}}^N V_{ij} \quad , \quad (4.2)$$

where  $V_{ij}$  is the interaction energy<sup>19</sup> between particles  $i$  and  $j$ . The system potential energy  $U_N$  [cf. Eq. (2.2)] is then given by

$$U_N = \frac{1}{2} \sum_{j=1}^N \epsilon_j \quad . \quad (4.3)$$

In Table II we show the variation of  $e = \langle U_N \rangle / N$  with separation of apolar species. No real trend in  $\langle U_N \rangle$  is discernible; in fact, the four values agree within the limits of the statistical errors. This is clearly due to the fact that  $U_N$  is dominated by the number (and strength) of water-water interactions far from the apolar species and thus does not change much with change in the separation of the apolar species. The hydrogen bond networks appear to adjust in such a way (with change of  $r_{ab}^0$ ) that no protons are left completely unbonded.

TABLE II. The average solvation energy and the average system potential energy for the four runs. The initial separation of the apolar species  $r_{ab}^0$  is shown in angstroms. Averages were performed over 1 080 000 configurations.

	A	B	C	D
$r_{ab}^0$ (Å)	3.87	5.27	6.08	6.60
$\langle e_{\text{sol}} \rangle^a$	-0.90	-0.92	-0.96	-0.99
$\langle e \rangle^b$	-10.37	-10.30	-10.24	-10.29

<sup>a</sup>In units of kcal/mole. Uncertainty typically  $\approx \pm 0.24$  kcal/mole.

<sup>b</sup>In units of kcal/mole. Typical uncertainty  $= \pm 0.15$  kcal/mole.

To analyze the changes introduced in the hydrogen bonding upon introduction of the apolar species, it is natural to subdivide the total number of solvent molecules into those constituting the hydration shell ( $N_S$ ) and those far removed from the apolar species to be termed bulk molecules ( $N_B$ ). A molecule of water was considered to be part of the hydration shell if its oxygen atom was within a distance  $R_S = 5.45$  Å from either of the apolar species. Because there is no universal agreement on the optimum value of  $R_S$ , we picked the distance  $R_S$  corresponding to the first minimum in  $g_{AO}(r)$ . It is very close to the value selected by Owicki and Scheraga,<sup>11</sup> but slightly larger than the value employed by Geiger *et al.*<sup>10</sup> In analogy to the analysis of the radial structure in terms of  $g_{AO}(r)$ , we defined the hydration shell as a hemisphere centered on one of the apolar spheres and pointing away from the second apolar species (see Fig. 2). The water molecules residing in the hemispheres pointing towards the second apolar species are considered to form the subset  $N_I$  (Fig. 2).

The average binding energy per molecule of the three subsets  $N_S$ ,  $N_B$  and  $N_I$  are defined as

$$\langle E_k \rangle = \left\langle \frac{1}{N_k} \sum_{i=1}^{N_k} \epsilon_i \right\rangle \quad (k=S, B, I) \quad (4.4)$$

TABLE III. Average binding energies for the shell ( $\langle E_S \rangle$ ), bulk ( $\langle E_B \rangle$ ) and intermediate ( $\langle E_I \rangle$ ) regions of the box. See Fig. 2 for definition of these regions. The average number of particles in these regions are also given, in rows 4–6.  $\langle V \rangle_B$ ,  $\langle V \rangle_S$  and  $\langle V \rangle_{S-B}$  represent the average pair energies for shell–shell, bulk–bulk, and shell–bulk pairs respectively.

	A	B	C	D	Typical uncertainty in our data	Geiger <i>et al.</i> , Ref. 6	Owicki and Scheraga, Ref. 7
$\langle E_B \rangle$	-20.83	-20.72	-20.54	-20.60	$\pm 0.22$	-19.79	-18.14
$\langle E_S \rangle$	-21.68	-20.91	-21.19	-21.58	$\pm 0.47$	-19.95	-18.82
$\langle E_I \rangle$	-21.55	-21.12	-21.12	-21.24	$\pm 0.73$	...	...
$\langle N_B \rangle$	185.06	182.03	176.90	178.20	$\pm 1.4$	196.1	77
$\langle N_S \rangle$	20.28	19.87	20.09	20.49	$\pm 1.2$	17.9	23
$\langle N_I \rangle$	8.66	12.07	15.91	15.31	$\pm 1.8$	...	...
$\Delta(\langle E_S \rangle - \langle E_B \rangle)$	-0.85	-0.18	-0.66	-0.98	$\pm 0.52$	0.16	0.68
$\langle V \rangle_B$	-2.87	-2.94	-2.92	-2.87	$\pm 0.05$	...	-3.52
$\langle V \rangle_S$	-3.93	-3.57	-3.66	-3.99	$\pm 0.12$	...	-4.02
$\langle V \rangle_{S-B}$	-3.34	-2.76	-2.85	-2.85	$\pm 0.15$	...	-3.63
$\Delta U$	-8.62	-1.79	-6.63	-10.04	$\pm 5.2$	-1.1	-7.68

where  $N_S + N_B + N_I = N_W$ , the number of water molecules in the system, and the ensemble average is evaluated as described in Sec. II. It is clear from Table III that the shell molecules are much more strongly bound than the bulk molecules, the difference  $\Delta(\langle E_S \rangle - \langle E_B \rangle)$  varies with the separation of the two apolar species, but it is on the order of 0.5 to 1.0 kcal/mole. Thus it is indeed very surprising that the shell molecules despite having a weak interaction with the apolar species are more strongly bound than the bulk molecules. It is interesting to note that case B in Table III displays a slightly different behavior from the others. This may be due to the fact (noted previously) that the separation  $r_{ab}^0$  for case B corresponds to a comparatively unstable position for the pair of apolar species. The difference  $\Delta(\langle E_S \rangle - \langle E_B \rangle)$  for this case turns out to be much smaller than in the other three cases, for reasons discussed below.

The row labeled  $\Delta U$  gives the energy change in water caused by dissolution of a mole of solute; we compute it from

$$\Delta U = (\langle N_S \rangle / 2) \Delta(\langle E_S \rangle - \langle E_B \rangle) \quad (4.5)$$

where  $\langle N_S \rangle$  is the average number of water molecules in the hydration shell. With the exception of case B, this quantity turns out to be approximately -8 kcal/mole solute (Table III), in reasonable agreement with the results of Owicki and Scheraga.<sup>11</sup> As we have remarked before, case B corresponds to the case when the two apolar species are at an unstable position with respect to their potential of mean force. The apolar species therefore make much larger excursions in configuration space in case B than in cases A, C, and D resulting in a less defined hydration shell for the former (case B). We believe it is because of this factor that  $\Delta U$  for B is much smaller than for A, C, or D. For comparison we note Rossky and Karplus<sup>20</sup> get a value of  $\Delta U = -3.6$  kcal/mole solute for the water molecules around the nonpolar part of a dipeptide, and Owicki and Scheraga<sup>11</sup> get a value of  $\Delta U = -7.82$  kcal/mole solute for the water molecules around a single methane molecule dissolved in water. In contrast, Geiger *et al.*<sup>10</sup> obtained a value

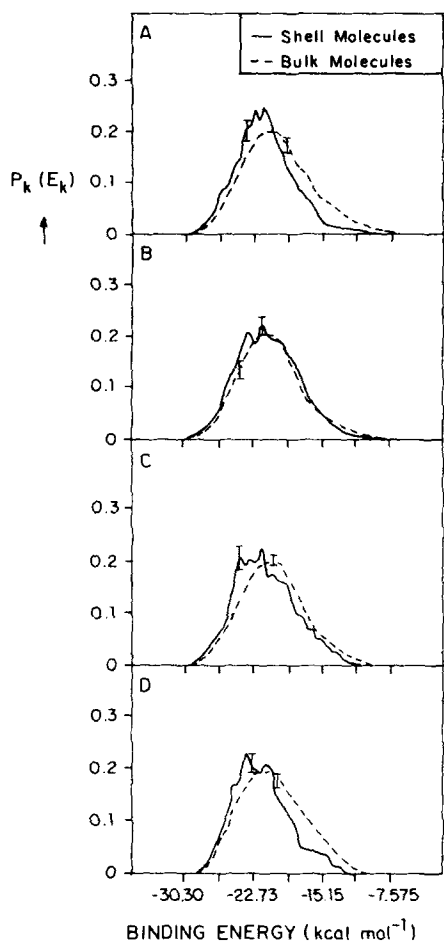


FIG. 7. Probability distribution function for water-water binding energies for molecules in the bulk and shell regions. The labels *A*, *B*, *C*, *D* refer to different initial separations of the pair of apolar species.

$\Delta U = -1.1$  kcal/mole solute for Ne atoms in water, a value that is significantly different from the above. It is difficult to account for this difference. Perhaps the  $\Delta U$  determined in the molecular dynamics simulation corresponds to states far from equilibrium. After all, these runs are on the order of 10 000 steps. During this time very few hydrogen bonds can be broken. It may take the water molecules in the vicinity of an apolar species considerable time to cool down.

To gain a better understanding of the energetics we report the probability distribution function  $P_k(E_k)$  for two of the subsets  $k=S, B$ .  $P_k(E_k)$  gives the probability of finding a state where the subset  $k$  has a binding energy per particle ( $E_k$  in the interval  $E_k \pm \Delta E/2$ ). In Fig. 7 we show  $P_S(E)$  and  $P_B(E)$  for the four cases *A*, *B*, *C*, and *D*. While all the distributions are broad, bell-shaped curves, those for the shell molecules are consistently narrower and peaked at lower values of  $E$ . Also, the curves for the shell molecules are not as smooth as those for bulk molecules because of poorer statistics for the former arising from  $N_S \ll N_B$ . Again we note the lack of a strong distinction between the bulk and shell molecules for case *B*. The average values of these functions,  $\langle E_k \rangle$ , have been discussed above [see Eq. (15) and

the paragraph following it].

The pair energy distribution function  $p_k(V)$  gives the probability of a pair of water molecules belonging to the subset  $k$  having an interaction energy in the range  $V + \Delta V/2$  to  $V - \Delta V/2$ . Only nearest neighbor interactions are considered, that is, between water molecules whose oxygen atoms are separated by a distance less than 3.50 Å. The pair energy  $V_{ij}$  for the pair  $(i, j)$  is considered for  $P_k(V)$  only if both  $(i, j)$  belong to the same subset  $k$ ; otherwise it is included in the distribution function  $P_{S-B}(V)$  for molecules comprising the boundary between the shell and bulk. Distribution functions determined in this manner are shown in Fig. 8. The distribution functions are seen to be broad and asymmetric. The mean values of these functions denoted by  $\langle v_k \rangle$  where  $k=S, B, S-B$  respectively denote the shell, or the bulk, or the boundary pairs of molecules, are reported in Table III. The difference between the shell and the bulk pair energies is quite large, in fact, much larger than is suggested by a comparison of the binding energies  $\langle E_k \rangle$ . One explanation of this apparent discrepancy is

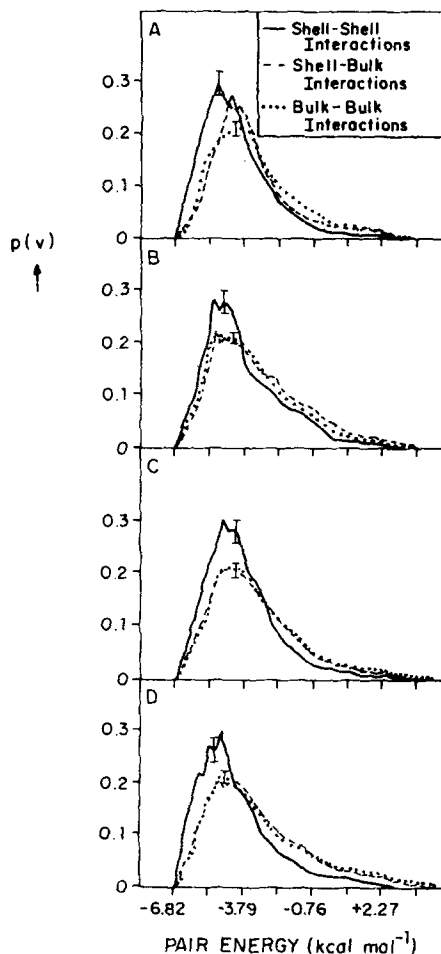


FIG. 8. Probability distribution functions for pair interaction energies  $V_{ij}$ . A pair energy  $V_{ij}$  for the pair  $(i, j)$  is considered for the shell distribution only if both  $(i, j)$  belong to the shell region and the pair is separated by less than 3.30 Å. Likewise, the bulk distribution counts only those nearest neighbor pairs which both belong to the bulk region. Pairs for which one member belongs to the shell and other to the bulk are considered in the distribution  $p_{S-B}(V)$ .

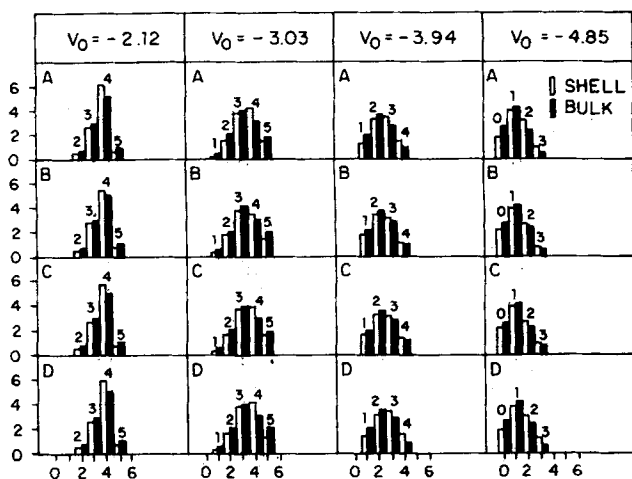


FIG. 9. Probability distribution function for the number of hydrogen bonds formed by a molecule. Results for bulk molecules are shown in hatched rectangles while those for shell molecules are indicated with clear rectangle.

that the shell molecules do lack one full water-water interaction because of the presence of the apolar species. The distribution function  $p_s(V)$  appears to consistently show a forklike structure in the peak, although this is within the statistical noise (as shown in Fig. 8).

In order to get a quantitative feel for the increase in hydrogen bonding in the shell compared to the bulk, a bond energy analysis for the number of hydrogen bonds formed by a molecule was performed. A pair of molecules  $i$  and  $j$  is designated to be hydrogen bonded if the interaction energy  $V_{ij}$  for the pair lies below a preassigned negative cut-off energy  $V_0$ . Just as in the determination of  $P_k(V)$  discussed in the preceding paragraph, the analysis for the number of hydrogen bonds was restricted to nearest neighbor molecules. The number of hydrogen bonds formed by each molecule was determined for various values of  $V_0$ . Then the fraction of molecules  $n_k(m)$ , from the subset  $k$  having exactly  $m$  hydrogen bonds ( $m=0, 1, 2, \dots$ ), was computed. The resulting fractions  $\{n_k(m)\}$  are displayed in Fig. 9. With a large choice for  $V_0$ , only very few pairs are counted as being hydrogen-bonded. We see that with such a choice for  $V_0$ , i.e.,  $V_0 = -3.94$ , or  $-4.85$  kcal/mole the fraction of molecules with three or more hydrogen bonds is larger for shell molecules (shown with unshaded rectangles in Fig. 9) than for bulk molecules (shaded rectangles). However, with a smaller choice for  $V_0$ , i.e.,  $V_0 = -2.12$  or  $-3.03$  kcal/mole, the bulk molecules engage in a larger number of hydrogen bonds. This is understand-

able since the shell molecules have fewer water molecules surrounding them due to the presence of the apolar species. To summarize, shell molecules engage in stronger hydrogen bonding than bulk molecules but there is one less water-water interaction at short range for the shell molecules. Rather similar conclusions were drawn by Geiger *et al.*<sup>10</sup> in their study of the hydration of Lennard-Jones spheres. As we pointed out in Ref. 13, the quantity  $n(m)$  which is the fraction of water molecules with exactly  $m$  hydrogen bonds in a system of pure ST2 water, depends on the boundary condition used in the simulation. Therefore, it is possible that differences on  $n_k(m)$  between shell and bulk molecules also depend on the boundary condition. Indeed it would be of interest to perform a study similar to one reported with a different boundary condition.

- <sup>1</sup>C. Tanford, *The Hydrophobic Effect* (Wiley, New York, 1973).
- <sup>2</sup>C. Pangali, M. Rao, and B. J. Berne, *J. Chem. Phys.* **71**, 2975 (1979), preceding paper.
- <sup>3</sup>A. Ben Naim, *Water and Aqueous Solutions* (Plenum, New York, 1974).
- <sup>4</sup>*Water, A Comprehensive Treatise*, edited by F. Franks (Plenum, New York, 1973).
- <sup>5</sup>E. V. Goldammer and H. G. Hertz, *J. Phys. Chem.* **74**, 3734 (1970).
- <sup>6</sup>R. Pottel and V. Kaatze, *Ber. Bunsenges. Phys. Chem.* **73**, 437 (1969).
- <sup>7</sup>H. S. Frank and M. W. Evans, *J. Chem. Phys.* **13**, 507 (1945).
- <sup>8</sup>L. Pratt and D. Chandler, *J. Chem. Phys.* **67**, 3683 (1977).
- <sup>9</sup>M. Rao, C. Pangali, and B. J. Berne, *Mol. Phys.* **37**, 1773 (1979).
- <sup>10</sup>A. Geiger, A. Rahman, and F. H. Stillinger, *J. Chem. Phys.* **70**, 263 (1979).
- <sup>11</sup>J. C. Owicki and H. A. Scheraga, *J. Am. Chem. Soc.* **99**, 7413 (1977).
- <sup>12</sup>S. Swaminathan, S. W. Harrison, and D. L. Beveridge, *J. Am. Chem. Soc.* **100**, 3255 (1978).
- <sup>13</sup>C. Pangali, M. Rao, and B. J. Berne, "A Monte Carlo study of structural and thermodynamic properties of water: Dependence on the system size and on the boundary conditions," *Mol. Phys.* (in press).
- <sup>14</sup>W. F. Van Grunsteren, H. J. Berendson, and J. A. C. Rullman, *Faraday Discuss. Chem. Soc.* **66**, 6614 (1978).
- <sup>15</sup>A. J. C. Ladd, *Mol. Phys.* **33**, 1039 (1977).
- <sup>16</sup>F. H. Stillinger and A. Rahman, *J. Chem. Phys.* **60**, 1545 (1974).
- <sup>17</sup>C. Pangali, M. Rao, and B. J. Berne, in "Computer Modeling of Matter," ACS Symposium series **86**, 32 (1978).
- <sup>18</sup>F. H. Stillinger, *J. Solution Chem.* **2**, 141 (1973).
- <sup>19</sup>For the pair of apolar species,  $V_{ij}$  does not include the harmonic potential  $U_H$ .
- <sup>20</sup>P. J. Rossky and M. Karplus, Preprint (1979).